

CHAPTER 7

CHARACTERIZATION OF MOLYBDENUM SULPHOSELENIDES - ELECTROLYTE INTERFACE

CONTENTS				PAGES
7.1	Introduction	129
7.2	Results and Discussions	130
7.2.1	Spectral response measurements		..	130
7.2.2	Capacitance measurements	134
7.3	Conclusions	137
	References	138

7.1 Introduction

Since the energy conversion efficiency of a solar cell device depends upon the optical band gap of semiconducting material and better energy conversion efficiency is obtained when the optical band lies in the range 1.1 to 2.1 eV¹⁻⁵). Various workers⁶⁻¹⁰) have attempted the preparation of solid solutions of two compounds and used them as photo-electrode materials. In general, the properties like band gap energy, band positions of a solid solution is dependent on its composition and is intermediate between that of the two components. Thus the suitable band gap material can be easily made available from appropriate composition of constituents. The importance of transition metal dichalcogenides as solar energy materials for efficient conversion of light energy to electrical or chemical energy has already been explained earlier. These materials form a wide range of solid solutions with either mixed metal or chalcogenide composition or both. Keeping this in view author has made attempts to fabricate the photoelectrochemical solar cells using the grown crystals of molybdenum sulphoselenides ($\text{MoS}_x\text{Se}_{2-x}$, $0 \leq x \leq 2$) and characterize them optically and electrochemically. Determination of optical band gap from spectral responses and flat band potentials in the present work on $\text{MoS}_x\text{Se}_{2-x}$ have been

made by capacitance measurements from Mott-Schottky plots.

7.2 Results and Discussion

7.2.1 Spectral response measurements

The experimental arrangement for the spectral response measurement of PEC cell is shown in Fig. 7.1. The arrangement consists of a grating monochromator (Central Electronic Ltd., India), PEC cell using molybdenum sulpho-selenide electrode and digital multimeter. The semiconductor electrode fabrication already has been described in the previous chapter. The electrolyte used in the present study was an aqueous iodine/iodide electrolyte, prepared by mixing 2 M NaI, 0.025 M I₂, 0.5 M Na₂SO₄ and 0.5 M H₂SO₄ in double distilled water. Platinum grid has been used as a counter electrode. PEC cell has been illuminated by monochromatic light from a monochromator and spectral response has been observed for wavelengths 910 nm to 500 nm at an interval of 10 nm.

The spectral dependence of the photocurrent of MoS_xSe_{2-x}, x = 0.05, 1.0, 1.5, 2.0 on the wavelength of incident light is shown in Fig. 7.2. In all cases the output photocurrent gradually drops toward the UV region although the light absorption in the semiconductor continues

to increase. The decrease in spectral response towards the long-wavelength region may be attributed to the fact that an increasing fraction of photons was absorbed beyond the region determined by space charge layer plus the diffusion length of holes, so that corresponding electron-hole pairs get lost by recombination¹¹⁾. The decrease in the spectral response at short wavelengths is due to the recombination in the surface region where recombination is highest. According to De Angelis et al¹²⁾ the wavelength dependence of photocurrent was explained by taking into account the depletion layer width, light penetration depth, and thickness of sample. It was suggested by Tributsch⁵⁾ that the photocurrent of transition metal dichalcogenides essentially arises from direct d-d transition.

The semiconductor-electrolyte interface can be treated as Schottky barrier³⁾ and the photocurrent has the following behaviour

$$J = e\phi_0 \left\{ 1 - \frac{\exp[-\alpha W_0 (V - V_{fb})^{1/2}]}{1 - \alpha L_p} \right\} \quad (7.1)$$

where ϕ_0 is the photon flux, L_p is the hole diffusion length, V_{fb} is the flat band potential, α is the optical absorption coefficient and W_0 is characteristic depletion layer width. W_0 is given by $(2\epsilon/e N_D)^{1/2}$ where

ϵ is the dielectric constant, e is the electronic charge and N_D the donor density.

It has been shown that the optical absorption for interband transitions in a semiconductor close to the gap behaves as

$$\alpha = \frac{A(h\nu - E_g)^{n/2}}{h\nu}, \quad (7.2)$$

where $n = 1$ for direct and $n = 4$ for indirect transitions. These two equations completely describe the photoresponse of the semiconductor-electrolyte junction.

It has been suggested by Lemasson et al¹³⁾ that the photoresponse is directly proportional to the photon flux and by Redon and Vigneron¹⁴⁾ that the photocurrent is proportional to absorption spectrum. The plots of $(Jh\nu)^2$ versus $h\nu$ (Fig. 7.3) for the compounds of molybdenum sulphoselenides, are straight lines ($n = 1$) indicating that these materials are direct band gap semiconductors. The values of optical band gaps obtained from $(Jh\nu)^2$ versus $h\nu$ plots have been shown in Fig. 7.4 and compared with other workers in Table 7.1, which shows good agreement. It has been observed that the band gaps of molybdenum sulphoselenides increase from 1.4 eV for MoSe_2 to 1.74 eV for MoS_2 .

- Fig. 7.1 Photograph of the experimental set up for spectral response measurements.
- Fig. 7.2 Plots of photocurrent versus wavelength for molybdenum sulphoselenides.
- Fig. 7.3 Plots of $(Jh\nu)^2$ versus $h\nu$ for molybdenum sulphoselenides.

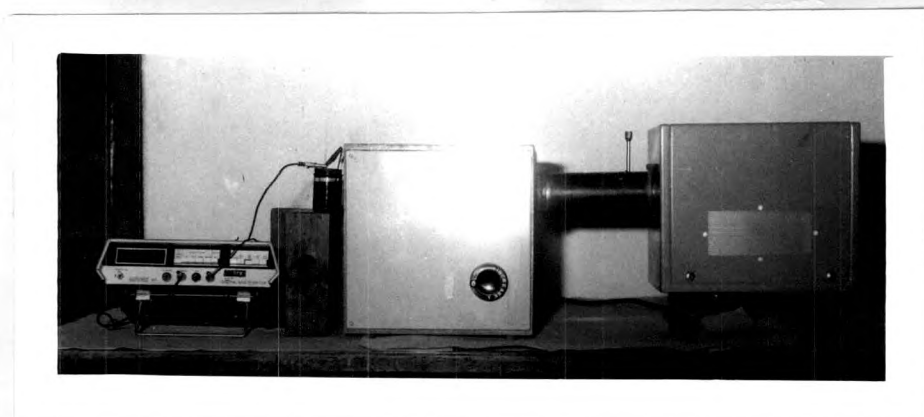


Fig. 7.1

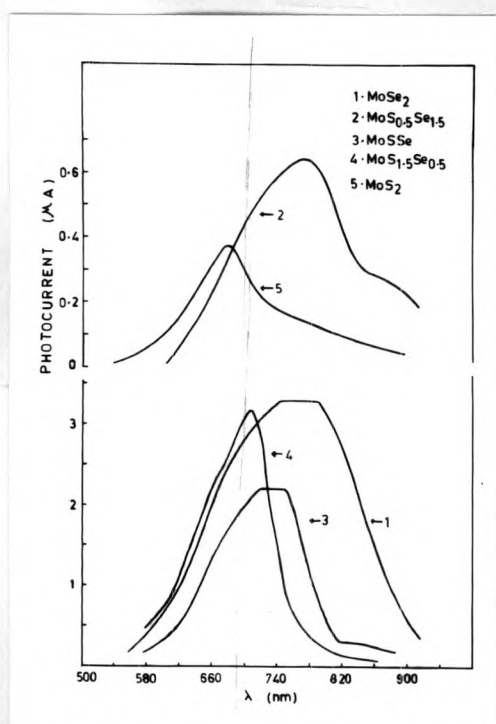


Fig. 7.2

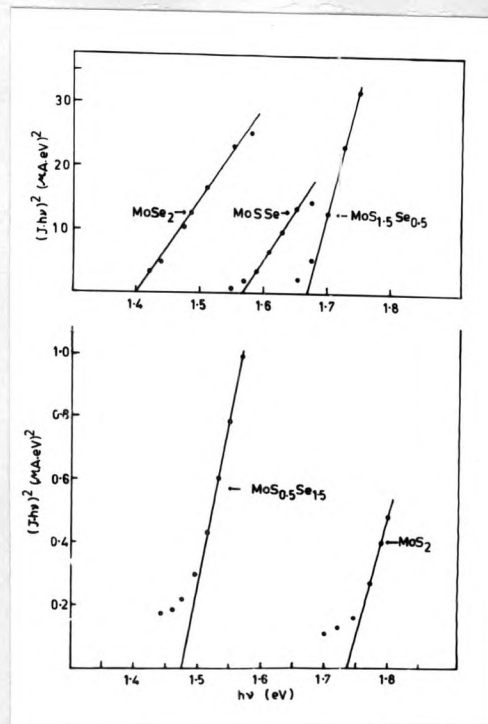


Fig. 7.3

Table 7.1Summary of band gap data for molybdenum sulphoselenides

Semiconductor	Band gap eV	
	Direct	
	This work	Literature
MoSe ₂	<u>1.4</u>	1.4 ^{5,15)} <u>1.38¹⁶</u> <u>1.36¹⁷⁾</u>
MoS _{0.5} Se _{1.5}	1.475	
MoSSe	1.57	
MoS _{1.5} Se _{0.5}	1.67	
MoS ₂	<u>1.74</u>	1.75 ^{5,18)} <u>1.77¹⁶⁾</u>

7.2.2 Capacitance measurements

For capacitance measurements method employed in Chapter 6 has been used.

Mott-Schottky plots of $\text{MoS}_x\text{Se}_{2-x}$ ($0 \leq x \leq 2$) electrodes are depicted in Fig. 7.5. The flat band potentials evaluated are found to be increasing from $V_{\text{SCE}} = -0.3$ V for MoSe_2 to 0.18 V for MoS_2 . Gerischer et al¹⁹⁾ also found the flat band potential in aqueous I^-/I_2 electrolyte as $V_{\text{SCE}} = -0.3$ V for MoSe_2 and 0.1 to 0.2 V for MoS_2 . However Chandra et al¹⁷⁾ have found flat band potential in aqueous I^-/I_2 electrolyte for the different thickness of electrodeposited MoSe_2 films as $V_{\text{SCE}} = -0.26$ V and -0.486 V. The variation of flat band potential with the composition of $\text{MoS}_x\text{Se}_{2-x}$ single crystals is shown in Fig. 7.6. The variation is linear with respect to x . The donor concentrations N_D have been determined from the slope of Mott-Schottky relation as,

$$N_D = 2 [e \epsilon \epsilon_0 (\text{slope})]^{-1} \quad (7.3)$$

where ϵ is the dielectric constant of the crystal. The dielectric constants of molybdenum sulphoselenides crystals have been evaluated using the relation $\epsilon = Cd/A\epsilon_0$ where C is the capacitance, d the thickness of the crystal and A

Fig. 7.4 Variation of direct band gap with the composition 'x' of $\text{MoS}_x\text{Se}_{2-x}$ series.

Fig. 7.5(a) Mott-Schottky plots of MoSe_2 , MoSSe , $\text{MoS}_{1.5}\text{Se}_{0.5}$ and MoS_2 in aqueous iodine/iodide solution.

Fig. 7.5(b) Mott-Schottky plots of $\text{MoS}_{0.5}\text{Se}_{1.5}$ in aqueous iodine/iodide solution.

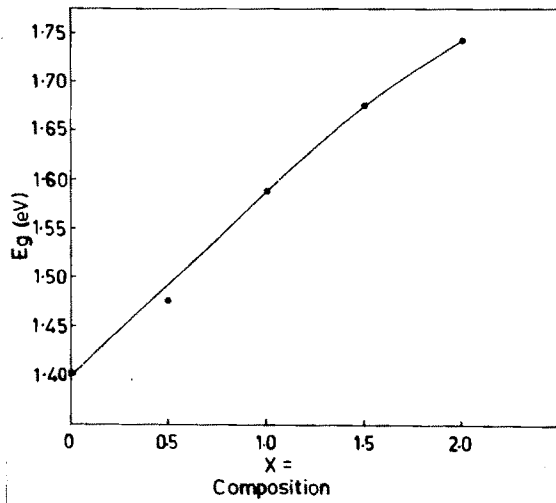


Fig. 7.4

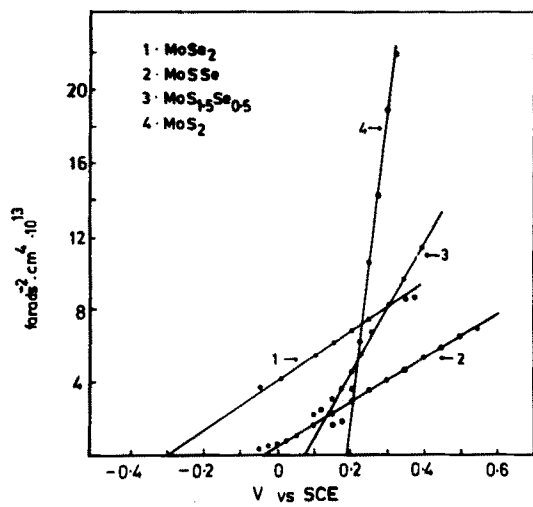


Fig. 7.5(a)

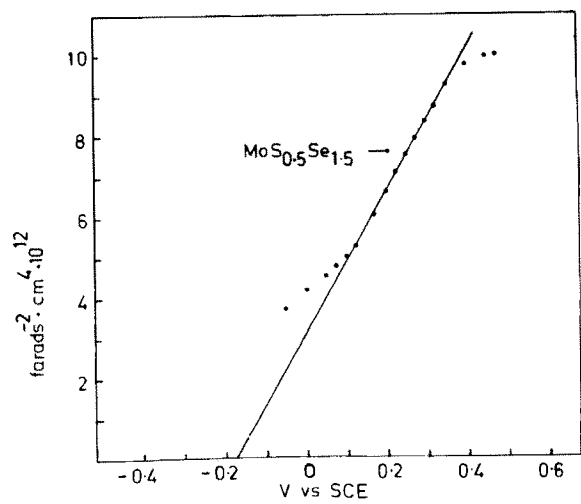


Fig. 7.5(b)

the area of contact. The dielectric constant for $\text{MoS}_x\text{Se}_{2-x}$ $0 \leq x \leq 2$ obtained is found to increase from 4.35 for MoSe_2 to 7.48 for MoS_2 as given in Table 7.2. The donor concentrations calculated using the above relations are also shown in Table 7.2.

The distance between conduction band minimum E_c and flat band potential V_{fb} is important to localize the valence band maximum.

According to Kautek and Gerischer²⁰⁾, in classical approximation where $(E_c - E_{fb})/kT > 1$, the effective density of conduction states is given by²¹⁾

$$N_C = \frac{2}{h^3} (2\pi m_e^* kT)^{3/2} \quad (7.4)$$

m_e^* is the effective mass of electron and is taken to be $0.5 m_e$ ²²⁾, m_e the electron mass, for transition metal dichalcogenides N_C comes out to be $8.8 \times 10^{18} \text{ cm}^{-3}$. Assuming that all donors are ionised and have given their electrons into the conduction band, we get the classical Maxwell Boltzmann distribution

$$E_c - E_{fb} = kT \ln N_C/N_D \quad (7.5)$$

Table 7.2

Data from the Mott-Schottky evaluations

Crystal	Dielectric constant ϵ	Donor concentration N_D cm^{-3}	$E_C - E_f$ V vs SCE	V_{fb} V vs SCE	E_V V vs SCE
MoSe ₂	4.357	2.498×10^{17}	0.093	-0.300	1.007
MoS _{0.5} Se _{1.5}	5.280	1.0354×10^{17}	0.115	-0.175	1.185
MoSSe	6.045	1.556×10^{17}	0.105	-0.040	1.44
MoS _{1.5} Se _{0.5}	6.837	9.292×10^{16}	0.118	+0.075	1.632
MoS ₂	7.4886	1.724×10^{16}	0.162	+0.180	1.758

$$(E - E_{fb}) = - e (V - V_{fb}) \quad (7.6)$$

Using these equations author has obtained the difference between the Fermi level and the edge of conduction band ($E_C - E_f$) for MoS_xSe_{2-x} as given in Table 7.2. By subtracting the band gap energy for molybdenum sulphoselenides given in Table 7.1, from the values of E_C , the conduction band, the valence band positions, E_V , have been located as depicted in Fig. 7.7. Fig. 7.7 suggests that the redox potentials (V_{redox}) within the gap i.e. positive of - 0.4 V and negative of 1.8 V vs SCE should be appropriate for PEC cells with molybdenum sulphoselenide electrodes.

7.4 Conclusion

The direct band gap of the grown series increases from 1.4 eV to 1.74 eV with the increasing sulphur content. The flat band potentials show an increasing trend in their value from the selenides to the sulphides of molybdenum. MoS_xSe_{2-x} ($0 \leq x \leq 2$) electrodes have been characterized in terms of the energetic location of the valence and conduction band positions, which suggest that the redox potentials within the gap, positive of - 0.4 V and negative of 1.8 V versus SCE should be appropriate for PEC solar cells of molybdenum sulphoselenides.

Fig. 7.6 Variation of flat band potential with the composition 'x' of $\text{MoS}_x\text{Se}_{2-x}$ in aqueous iodine/iodide solution.

Fig. 7.7 Positions of band edges of $\text{MoS}_x\text{Se}_{2-x}$ in aqueous iodine/iodide solution, CB, conduction band, VB valence band-edge, E_F Fermi level.

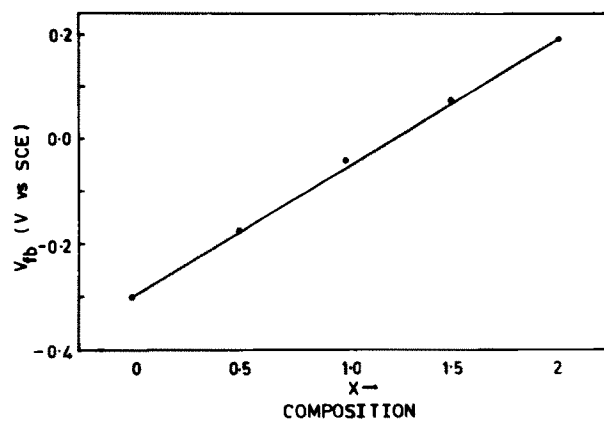


Fig. 7.6

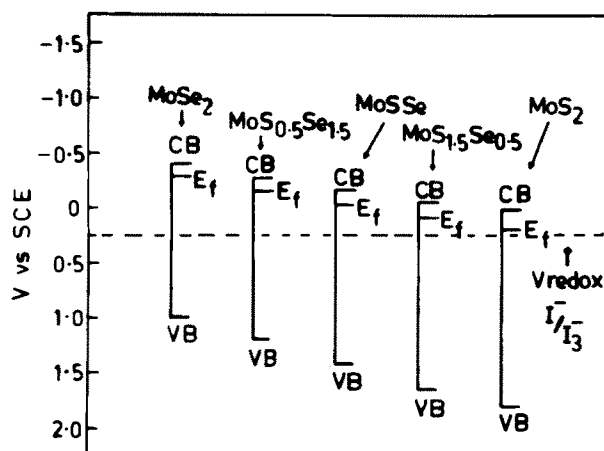


Fig. 7.7

References

1. Loferski, J. J. (1956)
J. Appl. Phys. 27, 777.
2. Noufi, R. and Warren, F. (1980)
SPIE Vol. 248, Role of Electro-optics
in P Photovoltaic Energy Conversion.
3. Butler, M. A. and Ginley, D. S. (1980)
J. Mat. Sci. 15, 1.
4. Sinha, A. P. B. (1983)
Energy Digest. Vol. 1, 1.
5. Tributsch, H. (1977)
Ber. Bunsenges. Phys. Chem. 81, 361.
6. Noufi, R., Kohl, P. and Bard, A. J. (1978)
J. Electrochem. Soc. 125, 375.
7. Hodes, G. (1980)
J. Electrochem. Soc. 127, 2252.
8. Redon, A. M. and Vigneron, J. (1980)
J. Electrochem. Soc. 127, 2347.

9. Karas, B. R. and Ellis, A. B. (1980)
J. Amer. Chem. Soc. 102, 968.
10. Sridevi, D. and Reddy, K. V. (1985)
Mat. Res. Bull. 20, 8, 929.
11. Van Merhaeghe, R. L. and Cardon, F. (1979)
Ber. Bunsenges Phys. Chem. 83, 236. ~~_____~~
12. De Anglelis, L., Scafe, E., Gulluzzi, F.,
Fornarini, L. and Scrosati, B. (1982)
J. Electrochem. Soc. 129, 6, 237.
13. Lemasson, P., Etcheberry, A. and
Goutron, J. (1983) =
Electrochimica Acta 27, 3, 607.
14. Redon, A. M. and Vigneron, J. (1981)
Solar Cells 3, 179.
15. Tributsch, H. (1978)
Ber. Bunsenges Phys. Chem. 82, 169.
16. Baglio, J. A., Calabrese, G. S., Kamieniecki, E.,
Kershaw, R., Kubiak, C. P., Ricco, A. J.,
Wold, A., Wrighton, M. S. and Zoski, G. D.
(1982)
J. Electrochem. Soc. 129, 7, 1461.

17. Chandra, S., Singh, D. P. Shrivastava, P. C.
and Sahu, S. N. (1984)
J. Phys. D. Appl. Phys. 17, 2125.
18. Tributsch, H. (1977)
Z. Naturforsch, Teil A 32, 972.
19. Gobrecht, J., Gerischer, H. and
Tributsch, H. (1978)
J. Electrochem. Soc. 125, 12, 2085.
20. Kautek, W. and Gerischer, H. (1980)
Ber. Bunsenges. Phys. Chem. 84, 645.
21. Gerischer, H. (1961)
Adv. Electrochem. Engang. 1, 139.
22. Wilson, J. A. and Yoffe, A. D. (1969)
Adv. Phys. 18, 193.